

Optimization of Spray Drying Conditions for Yield, Particle Size and Biological Activity of Thermally Stable Viral Vectors

Daniel A. LeClair¹, Emily D. Cranston¹, Zhou Xing², Michael R. Thompson^{1,*}

¹Department of Chemical Engineering, McMaster University

Hamilton, Ontario, Canada L8S 4L7

²McMaster Immunology Research Centre & Department of Pathology and Molecular Medicine,

McMaster University

Submitted to: Pharmaceutical Research

May 2016

* Author to whom correspondence should be addressed.

Email: mthomps@mcmaster.ca

Tel: (905) 525-9140 x 23213

Optimization of Spray Drying Conditions for Yield, Particle Size and Biological Activity of Thermally Stable Viral Vectors

Daniel A. LeClair¹, Emily D. Cranston¹, Zhou Xing², Michael R. Thompson^{1,*}

ABSTRACT

Purpose This work examines the relevance of viral activity in the optimization of spray drying process parameters for the development of thermally stable vaccine powders. In some instances, the actual active pharmaceutical ingredient (API) is not included in the process optimization as it is deemed too costly to use until the final selection of operating conditions, however, that approach is inappropriate for highly labile biopharmaceutics. We investigate the effects of spray drying parameters on i) yield, ii) particle size and iii) viral vector activity of a mannitol/dextran encapsulated recombinant human type 5 adenoviral vector vaccine, to demonstrate the effects and magnitude of each effect on the three responses, and further show that the API must be included earlier in the optimization.

Methods A design of experiments approach was used with response surface methodology (RSM) to optimize parameters including inlet temperature, spray gas flow rate, liquid feed rate and solute concentration in the feed.

Results In general, good conditions for maintaining viral activity led to reduced yield and fewer particles of the desired size. Within the range of parameters tested, the yield varied from 50%–90%, the percentage of ideally size particles was 10%–50%, and the viral vector titre loss was 0.25-4.0 log loss.

Conclusions RSM indicates that the most significant spray drying parameters are the inlet temperature and spray gas flow rate. It was not possible to optimize all three output variables with one set of parameters, indicating that there will only be one dominant criteria for processing which in the case of viral vaccines will likely be viral vector activity.

KEYWORDS: spray dry, adenovirus, viral vector, particle size, titre, yield, process parameters, surface response methodology, optimization

ABBREVIATIONS

API	active pharmaceutical ingredient
AdHu5LacZ	recombinant human type 5 adenoviral vector expressing <i>Escherichia coli</i> β -galactosidase
F	liquid feed rate
F _{1-5μm}	percentage of particles suitable for dry powder inhalation (1 - 5 μ m size)
M _r	relative molecular mass
Pe	Peclet number
RSM	response surface methodology
S	solute concentration in the liquid feed
SEM	scanning electron microscopy
SG	spray gas flow rate
T	titre log loss
TE	inlet temperature
T _g	glass transition temperature
We	Weber number
Y	powder yield

1. INTRODUCTION

Thermal sensitivity in biopharmaceuticals ranging from antibiotics to viral vectors remains a major problem today [1–3]. Diminished pharmacological activity notably occurs at moderate temperatures through chemical degradation and protein denaturation for these drug candidates [4,5]. Maintaining efficacy often demands adherence to *cold chain* storage and handling

protocols, which increase the cost of the drug to patients and complicates widespread distribution when refrigeration is required [6]. As a result, it has become a global challenge to increase the thermal stability of many active pharmaceutical ingredients (APIs) to ease logistic concerns. The vector platform used in this paper is a human type 5 adenovirus (AdHu5) encoding LacZ for *in vitro* detection of activity. It is known that thermally unstable APIs lose activity even at -20°C [7,8]. The AdHu5LacZ vector is commonly used as a model biological within vaccination studies [9,10]. Normal storage protocols for AdHu5 vectors require temperatures of -80°C, thus it is a suitable biologic to model processing aspects of developing a thermally stable vaccine. Vitrification methods which are suitable for increasing the thermal stability of a biologic aim to allow storage at much greater temperatures, such as 2-8°C or possibly even ambient temperature.

Vitrification of biologics within excipient matrices can enhance stability and is achieved through methods such as lyophilisation or spray drying. Lyophilisation has traditionally been preferred for handling biologics in order to completely avoid exposure to elevated temperatures during processing though it can be a more expensive process [11]. Spray drying has received far less attention with biologics, but the growing research on thermally stable vaccines and focus by companies on continuous processes has increased interest in the method. However, it can be a costly process as well, based on equipment installation, maintenance and scale-up in accordance with cGMP requirements [12]. The attractive feature for spray drying in the area of thermally stable vaccine production are its robustness, scalability, and continuous nature for producing particulate-form pharmaceuticals [13–15]. It is used for the manufacture of numerous solid oral dosage forms due to its continuous nature, short residence time, excellent particle size control, and low cost [13,16,17]. Furthermore, spray drying has been shown to provide reasonable scalability from the lab to industrial-scale processes [18].

The process dries biologics within glass-forming ingredients to create particles whereby these therapeutic actives are immobilized in stabilizing matrices. Biologics maintain stability throughout the drying process as the added excipients are typically able to replace stabilizing bonds between the water and biologic [19]. These stabilizing matrices can consist of sugars, sugar alcohols, amino acids, and surfactants, as they effectively replace the water-stabilizing bonds of isolated biomolecules while moisture is removed from the system throughout the drying process [20]. The high glass transition temperatures of these matrix species (often $T_g > 100^\circ\text{C}$) restrict molecular movement to the degree that aggregation of an API, such as a vaccine platform, is not possible [21]. The entrapped biologic within a stabilizing matrix is prevented from degrading and as a result, retains a higher activity after storage in moderate temperature environments. Previously, this has been demonstrated with a mannitol/dextran blend stabilizing AdHu5LacZ at storage temperatures as high as 55°C [15].

Spray drying is less commonly used for labile ingredients in the face of other approaches such as lyophilisation for drying APIs, never properly considering the short residence time and thermal environment within sprayed droplets. As a result, little process understanding exists to meet the stated global challenges [22] of producing thermally stable vaccines by spray drying methods. Earlier studies related to the present work have specifically optimized the yield and particle size of spray dried particles [23–26]. Further work has examined the effects of spray drying process parameters on various species of bacteria [27–29]. Understandably, viral vectors, as considered in the present work, exhibit different stabilizing profiles than that of bacterial biologics and have not been included in previously published optimization studies. Viral vector stability is influenced not only by thermal damage, but is also subject to destabilization through other methods such as hydrophobic interactions or spatial position within a formed particle [15].

This paper will examine the main operational variables to spray drying a thermally stable vaccine platform based on AdHu5LacZ, though with the intent of highlighting the necessity of measuring viral vector activity, in conjunction with more traditional spray drying responses such as powder yield and particle size, during optimization. To the best of our knowledge, this work is novel and considers the optimization of viral vector activity through spray drying for the first time. Viral vector stability must be thoroughly examined during preliminary spray drying trials instead of focusing on yield or particle size, which has been observed in previous studies [30–33]. This work argues for the viral vector to be included in the optimization trials despite the high expense.

2. MATERIALS AND METHODS

2.1. Chemicals and Adenoviral Vectors

D-mannitol and dextran (M_w 40,000 kDa) were purchased as USP grades from Sigma-Aldrich (Ontario, Canada). Culture media was produced from α -minimum essential medium (prepared in the lab according to protocol by the supplier, Life Technologies; Ontario, Canada) with 10% fetal bovine serum and 1% streptomycin/penicillin (Invitrogen; Ontario, Canada). X-Gal stock solution was purchased from EMD Millipore (Ontario, Canada). A recombinant replication-defective human type 5 adenovirus expressing *Escherichia coli* β -galactosidase (AdHu5LacZ) was produced in the vector facility of McMaster Immunology Research Centre as described previously [34].

2.2. Spray Drying, Process Parameters and Response Criteria

Powders were produced from spray drying with a Mini Spray Dryer B-290 (Büchi; Switzerland). The spray dryer was equipped with a 0.7 mm spray nozzle and high performance cyclone. The pressurized spray gas was dried and filtered using an in-line silica gel desiccant air dryer (McMaster-Carr; Elmhurst, IL) and Aervent® 0.2 μm filter (EMD Millipore; Billerica, MA). The feed solution was composed of mannitol and dextran – both FDA-acceptable excipients (at a weight ratio of 67% mannitol and 33% dextran) along with the AdHu5LacZ vector (1.5×10^6 pfu). Previously we demonstrated that the T_g for this formulation was 130°C and that the thermal stability of AdHu5LacZ was superior with mannitol/dextran compared to other sugars and amino acids [15]. The stabilization of viral vectors by vitrification within a glassy matrix is well known but depends on the API; we believe this binary mixture is a particularly good example for AdHu5 but other glassy formulations, such as sucrose/trehalose or lactose/trehalose may be suitable and the results of this RSM are applicable to other formulations. Feed solute concentrations within this study were lower than the maximum that can be achieved due to the low amount of the AdHu5 vector used. It is disadvantageous to have a high powder excipient to viral vector ratio as this is troublesome for reconstitution and therapeutic delivery of the spray dried formulation. The aspirator rate was fixed at 35m³/h for each case.

Adjusted process parameters in the study were inlet temperature (TE), gas flow rate (SG), liquid feed rate (F), and the solute concentration in the feed liquid (S). These process parameters were chosen as they were directly adjustable within the spray dryer process and anticipated to have the greatest effect due to previous reports within the literature [35,36]. Although the actual chamber temperature is important to the drying process, it is a correlated variable with many of the parameters tested and hence was not suitable to study. The parameter values used throughout

the optimization study are shown in Table 1, with each individual run listed; each parameter was studied at three levels to consider non-linear effects on the process. Optimization was performed based on the response criteria of (i) increasing the cumulative size fraction of spray dried particles in the range of 1-5 μm which are suitable for dry powder inhalation ($F_{1-5\mu\text{m}}$), (ii) maximizing the overall powder yield (Y) and (iii) minimizing AdHu5LacZ titre log loss (lost bioactivity) as a result of spray drying (T); the rank of importance given to each response variable will be discussed later.

Table 1. Design of Experimental Runs Examining Spray Drying Parameters.

Run	Inlet Temperature (°C)	Gas Flow Rate (L/h)	Liquid Feed Rate (mL/h)	Solute Concentration (% w/w)
1	0	0	0	0
2	-	+	-	+
3	0	0	0	0
4	-	+	-	-
5	+	+	-	-
6	-	+	+	+
7	+	-	-	-
8	+	+	+	+
9	0	0	0	0
10	-	-	-	-
11	+	+	-	+
12	-	-	+	-
13	-	+	+	-
14	+	+	+	-
15	+	-	+	-
16	+	-	+	+
17	-	-	-	+
18	0	0	0	0
19	-	-	+	+
20	+	-	-	+
21	-	0	0	0
22	+	0	0	0
23	0	-	0	0
24	0	+	0	0
25	0	0	-	0
26	0	0	+	0
27	0	0	0	-
28	0	0	0	+

2.3. Imaging of Spray Dried Powders

The spray dried particles without viral vector were examined using a JEOL JSM-7000F scanning electron microscopy (SEM, JEOL Ltd., Japan). Previous examination has shown the powders to retain the same size and morphology with viral vector included [15]. Furthermore, the morphologies of spray dried particles at specific inlet conditions was reproducible with viral vector present (see Supplementary Information). Powder samples were mounted with double-sided tape and sputter-coated with approximately 5 nm of gold. Micrograph images were collected at a working distance of 10.0 mm to 10.3 mm and an electron accelerating voltage of 5.0 kV. Electron microscopy was performed at pressures below 5.0×10^{-4} Pa. Resulting images were analyzed using ImageJ software [37].

2.4. Sizing and Yield of Spray Dried Powders

Particle size was determined using a Malvern Mastersizer 2000 (Malvern Instruments, United Kingdom) equipped with a He-Ne laser. The powders were suspended in anhydrous ethanol at concentrations of 1.0 mg/mL. Tested powders did not include viral vector as it was confirmed through a few select samples that the inclusion of viral vector had no effect on measured particles size or morphology (see Supplementary Information Figures S1-S4). It was found through analysis of scanning electron microscopy images that the morphology and size of spray dried particles did not differ through the inclusion of viral vector for the formulation chosen in this study [15]. A representation of ideal particle size with a Feret diameter between 1-5 μm was based on the cumulative weight fraction, $F_{1-5\mu\text{m}}$, in the desired size range quantified as a percentage. This size range represents the suitability of the powder sample for intranasal pharmaceutical delivery as this size offers the best penetration into the lungs [38]. The first

moment (i.e. d_{50}) of the size distribution was not considered as an appropriate optimization parameter in this study as some spray drying conditions produced such coarse particles that a bimodal distribution was found which inappropriately skews the average [39]. Choosing an interval size and accounting for the percentage of particles within that range was considered a more accurate manner to optimize the process and the size range chosen is identified as suitable for pulmonary delivery.

Powder yield was calculated simply as the mass of the powder out of the spray dryer divided by the mass of excipients originally spray dried multiplied by 100.

2.5. *In Vitro* Testing of Spray Dried Particles

2.5.1. Culturing of A549 Cells

A549 lung epithelial cells stored in liquid nitrogen were thawed. Cells were cultured with complete α -MEM in T150 flasks. The cell culture flasks were incubated in a Forma Series II Water Jacketed CO₂ Incubator (Thermo Scientific Corporation; Waltham, MA) at 37.0°C and 5.0% CO₂. When cells reached 80-90% confluency, they were either split to a new culture flask or plated in a 96-well plate for *in vitro* testing.

2.5.2. Spray Dried Formulation Viral Infectivity (Titre Log Loss)

Spray dried powders containing AdHu5LacZ were dissolved in culture media and then added to 96-well plates containing A549 lung epithelial cells for *in vitro* testing. Eight-fold serial volume dilutions were created at dilutions of 10^0 to 10^{-7} of the reconstituted sample. The A549 lung epithelial cells were incubated with the AdHu5LacZ dilutions for 24 hours. Afterward, the cells were fixed with a 0.2% glutaraldehyde (Sigma Aldrich)/0.8% formaldehyde (Sigma Aldrich)

solution in phosphate buffered saline (%v/v) for less than five minutes. The fixative was removed, and viral activity was detected using the X-gal color reaction with 5-bromo-4-chloro-3-indoyl β -(D)-galactoside. Cells positive for LacZ transfection were observed with an Axiobert 25 inverted light microscope (Zeiss, Germany). The resulting median tissue culture infectious dose (TCID₅₀) was calculated using the Reed-Muench method [40]. This end titre was compared with the initial titre to determine total titre loss from spray drying.

2.6. Data Analysis

The optimization study was produced using a Box-Wilson Central Composite Design response surface methodology within Design-Expert 7.0 (Stat-Ease, Minneapolis, MN). The experimental design was set up with the four process parameters at three levels, as discussed in Section 2.2. Three replicates were included for the center point to evaluate uncertainty. The initial factorial trials were performed in a random order to minimize bias. Data was analyzed through RSM and all statistical plots were created using the statistical package R (R Foundation for Statistical Computing, Austria). RSM models were calculated as surface plots of best fit to the experimental data. Each model was statistically significant ($p \leq 0.01$), indicating that each response was affected by the tested process parameters. Process parameters were determined to be statistically significant at $p \leq 0.05$, thus process parameters and parameter interactions that did not meet this criteria ($p > 0.05$) were not included in the model.

3. RESULTS

To represent the significance of each process variable to the responses of the weight fraction of particles with the desirable size, powder yield and viral vector titre log loss, a linear

regression model was constructed. An ideal optimized set of process conditions from the standpoint of being industrially relevant, would see vaccine powders produced with $F_{1-5\mu m} > 95\%$, $>85\%$ powder yield and less than 1 log loss; the goal of the program was to ultimately develop a thermally stable tuberculosis vaccine intended to be administered by dry powder inhaler. Each response was defined in Section 2. The three response surfaces corresponding to the selected process variables are given in Table 2.

Table 2. Response Surfaces for the Spray Drying of Mannitol/Dextran Particles Containing AdHu5LacZ.

Response variable	Expression*	Eqn.
$F_{1-5\mu m}$ (%)	$F_{1-5\mu m} = 25.89 - 3.94TE + 8.68SG - 2.60F - 8.87S - 1.02TE \cdot F + 5.64SG \cdot S - 6.90TE \cdot TE + 9.60F \cdot F$	(1)
Powder Yield (%)	$Y = 82.34 - 6.80TE - 2.93F - 3.54S - 6.02TE \cdot F + 17.81TE \cdot S + 21.44F \cdot S - 14.08F \cdot F$	(2)
Titre Loss (log)	$T = 0.99 + 0.67TE + 0.81SG - 0.011F - 0.92S + 0.79F \cdot S + 1.76SG \cdot SG$	(3)

* Spray drying process parameters: inlet temperature (TE), spray gas flow rate (SG), liquid feed rate (F) and solute concentration (S).

3.1. Percent of Ideally Sized Particles ($F_{1-5\mu m}$)

In examining the effect of spray drying parameters on $F_{1-5\mu m}$, all four parameters were found to be significant terms of the surface response model (Equation 1 in Table 2) along with the second order terms of TE•TE and F•F, and the two-way interactions of SG•S and TE•F.

The effect of each parameter on $F_{1-5\mu m}$ is shown in the given surface plots in Figure 1. $F_{1-5\mu m}$ was found to be as low as 10% and as high at 45% in the study but never approached the ideal case (i.e. $>95\%$). The second-order effect of inlet temperature meant that a maxima occurred for $F_{1-5\mu m}$ at moderate temperatures. Conversely, the second-order effect of liquid feed rate meant that a minima occurred for $F_{1-5\mu m}$ within the range of tested rates. Increasing the solute concentration reduced $F_{1-5\mu m}$ while increasing the gas flow increased $F_{1-5\mu m}$. These trends agree with previous observations by Elversson et al., where increasing solids content increased

the resulting particle size, and increasing the spray gas flow rate reduced the formed spray droplets[38].

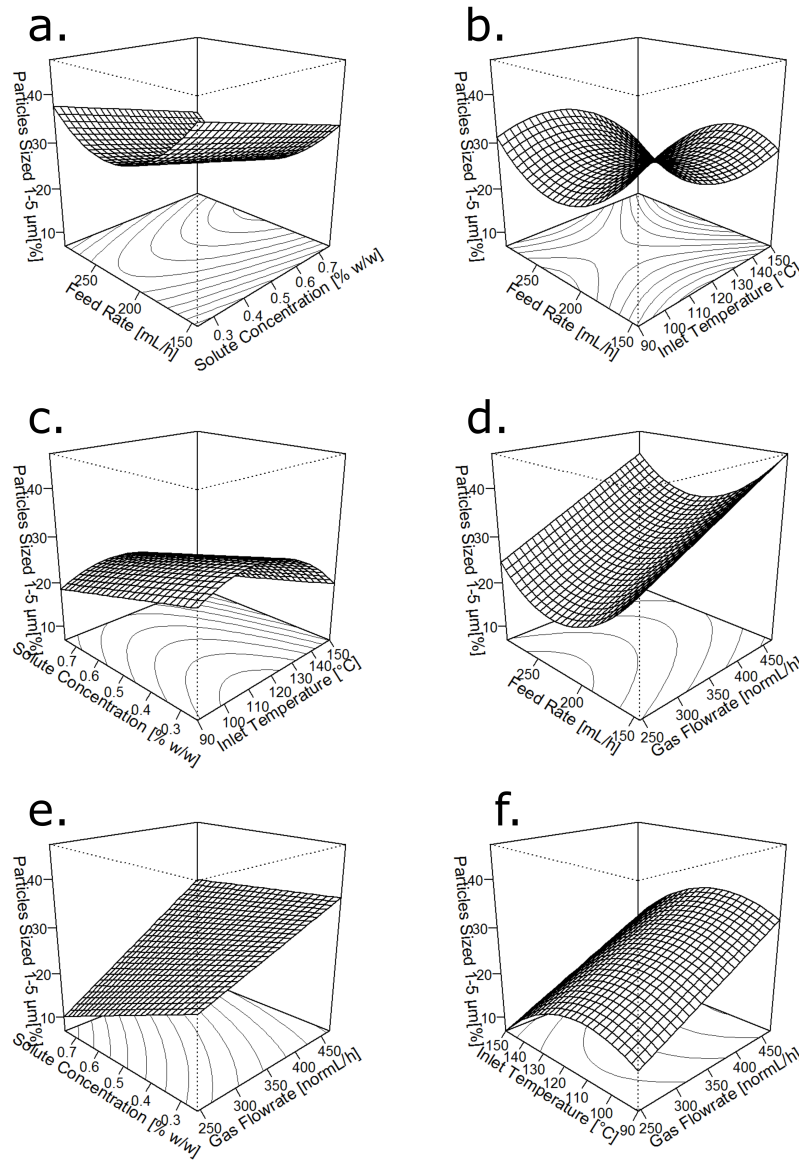


Figure 1. Surface plots for statistical model (Equation 1, Table 2) of percentage of particles sized 1-5 μm (%) against all process parameters.

3.2. Powder Yield

The significant main model terms for spray drying powder yield were TE and S, whereas the significant second order term was F•F, and two-way interactions were TE•S, F•S, and TE•F.

The model of surface response for powder yield is given as Equation 2, in Table 2. Powder yield ranged from > 90% to 50% within this study.

Surface plots in Figure 2 show the influence of each spray drying process parameter on powder yield. Inlet temperature exhibited a complex influence on powder yield by being correlated with solute concentration and feed rate, often producing a maxima in the range of 120°C. A lower yield was produced using a higher solute concentration for the matrix ingredients dissolved in the supplied liquid. The solute concentration and feed flow rate interacted positively on yield; the same was true for the interaction between inlet temperature and solute concentration. Maury et al. have previously reported on the influence of spray dryer parameters on powder yield, observing a decrease in powder yield at high inlet temperatures and increased liquid feed flow rates[23].

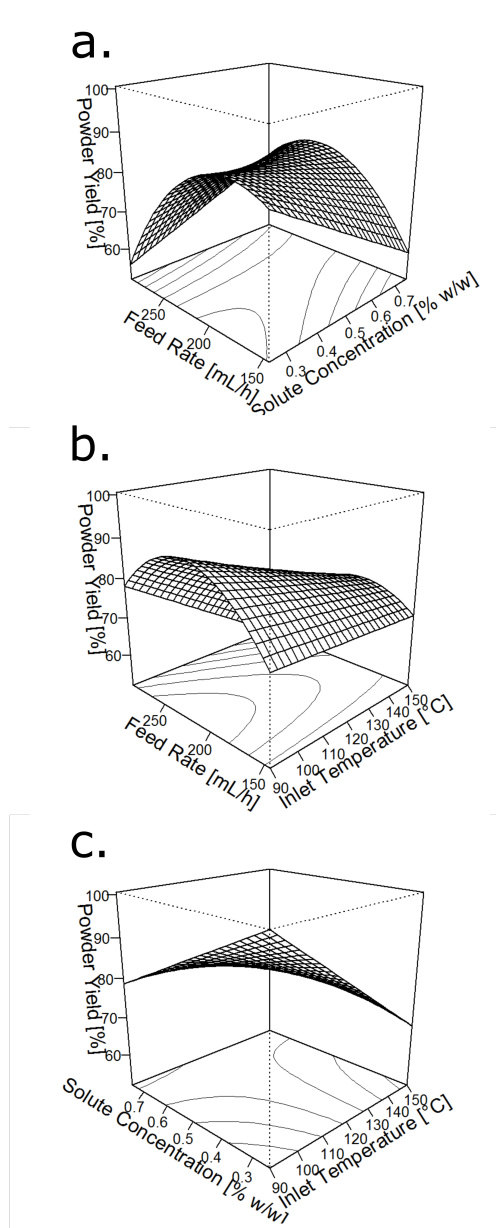


Figure 2. Surface plots for statistical model (Equation 2, Table 2) of powder yield (%) against all process parameters.

3.3. Titre Loss

The computed response surface for titre loss is given by Equation 3 in Table 2. The main model terms determined to be significant ($p \leq 0.05$) were TE, SG, S, while the significant

second-order effect was SG•SG and the two-way interaction was F•S. Their adjustment over the range of levels tested significantly altered the resulting total titre loss.

Surface plots modeling the effects of process parameters on total titre loss are shown in Figure 3; the lowest titre loss was sought in this study (corresponding to the highest retained bioactivity). The titre loss varied from less than 0.5 log loss to 4.0 log loss compared to the original viral vector stock (control). This implied that there is a wide range of spray drying parameters that can lead to viable APIs where less than 1 log loss is considered good but greater than 2 log loss is poor. The chosen surfaces in Figure 3 demonstrate the influence of the significant processing parameters on the resulting viral vector titre in the collected powders. The total titre loss for the adenovirus-containing powder was reduced by increasing the solute concentration within the liquid feedstock but was increased at high gas flow rate and high inlet temperatures. The feed rate generally did not influence the resulting viral vector titre loss except when correlated with changes in the solute concentration. In these cases, a higher feed rate minimized the negative outcome of lowering the solute concentration. Previously, work has examined the effects of spray dryer parameters on recovery of bacterial cells, particularly in the food industry [27–29]. The results within this work extend upon this through the use of a viral vector, for which stabilizing profiles differ from that of a bacterial cell.

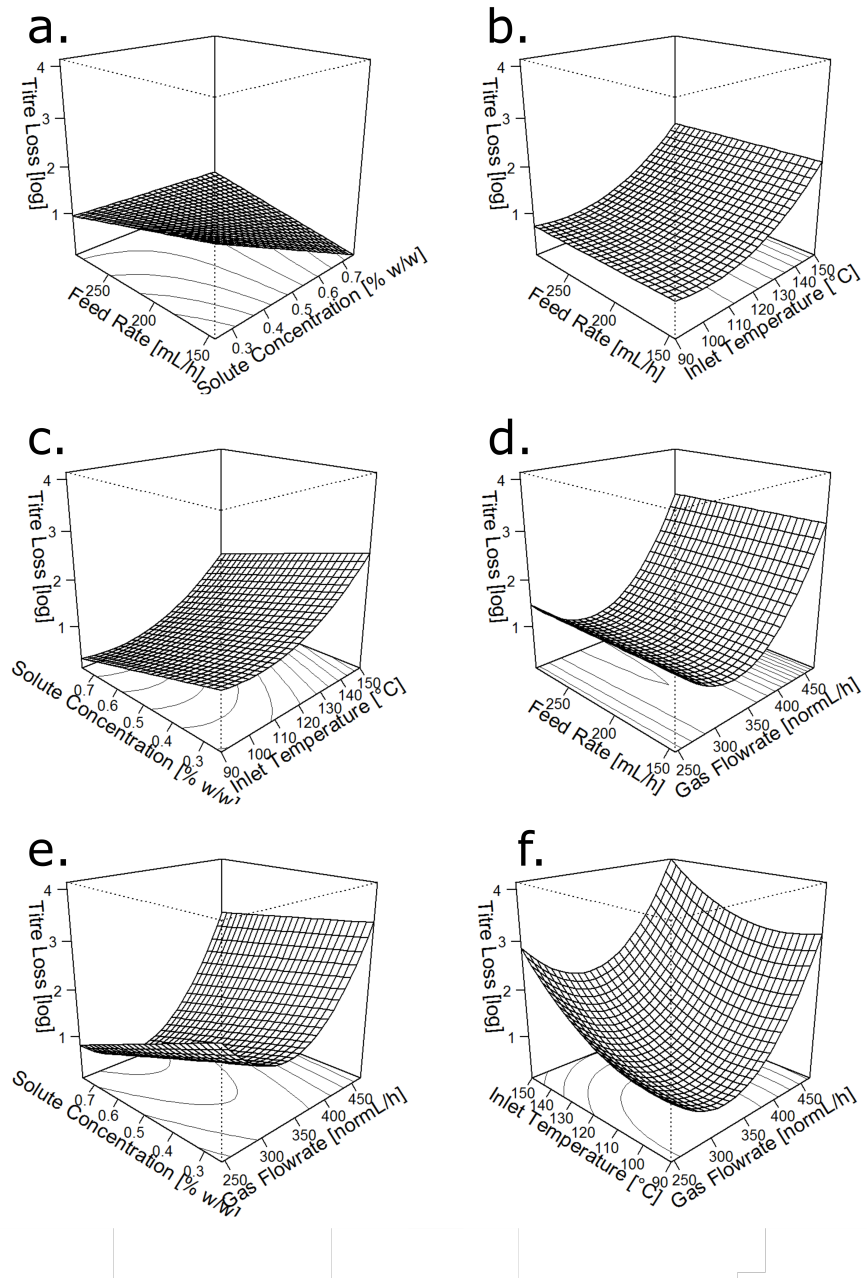


Figure 3. Surface plots for statistical model (Equation 3, Table 2) of AdHu5LacZ total titre loss (log) against all process parameter combinations.

4. DISCUSSION

4.1. Process Parameter Effects on Particle Size ($F_{1-5\mu\text{m}}$)

Typically, the low-end tail of the particle size distribution extends into the 1-5 μm range ($F_{1-5\mu\text{m}}$); the dominant proportion of particles are much larger than the identified ideal size range sought in this study. Examples of two distinctly different size distributions observed are given in Figure 4 with the fraction of particles contributing to $F_{1-5\mu\text{m}}$ highlighted. These different distribution shapes can arise, for example, from the collapse and breaking of spray dried particles which Figure 4b represents.

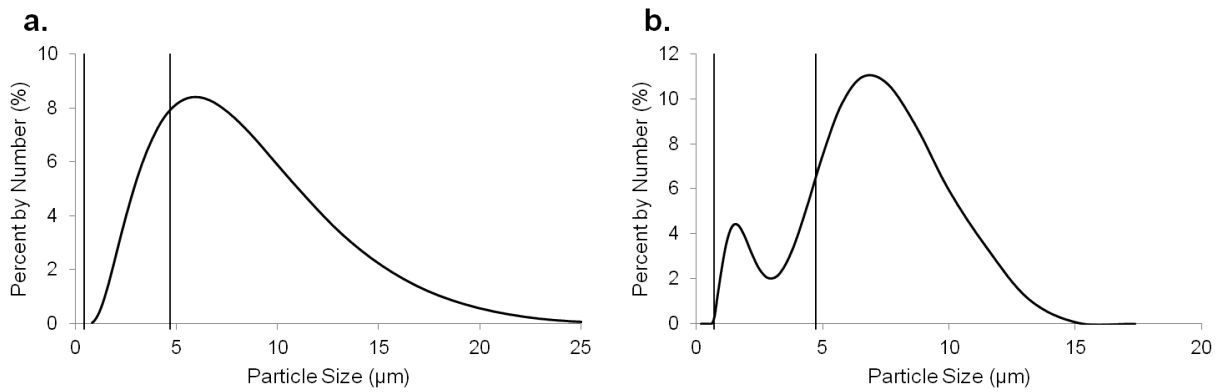


Figure 4. Particle size distributions of two trials are shown with the ideal size range ($F_{1-5\mu\text{m}}$) outlined by the vertical black lines. Distribution (a) presents a typical size distribution formed from non-collapsing particles (Run 2) whereas (b) shows a size distribution formed from collapsing and breaking particles (Run 6).

Inlet temperature of the spray dryer exhibits a second-order relationship with $F_{1-5\mu\text{m}}$ (Figures 1b, c, f) where the highest and lowest temperatures tested produce a lower amount of particles in the desired size range of 1-5 μm . At the higher end of the tested temperature range, particle temperature approaches the glass transition temperature of the matrix species and coalescence based on bridge formation between particles becomes possible, as observed in Figure 5 [41]. Furthermore, the high Peclet (Pe) number corresponding to these drying

conditions leads to a higher likelihood of larger sized (yet hollow) individual particles since surface solidification occurs much faster than solute diffusion within the droplet [42]. The Pe number given in Equation 4 represents the balance of evaporation rate (κ , Equation 5) versus solute diffusion, D_i in this process [43]:

$$Pe = \frac{\kappa}{8D_i} \quad (4)$$

$$\kappa = hA(T - T_\infty) \quad (5)$$

where the evaporation rate is increased by a larger temperature gradient between the drying droplet (T) and the air in the spray drying chamber (T_∞). The evaporation rate is also related to the convective heat transfer coefficient of the process (h) and the surface area of heat transfer (A). Thus, increasing the inlet temperature of the spray dryer increases drying and the formation of large, hollow particles, which is characterized by a greater Peclet number. The creation of hollow particles through spray drying often occurs using matrix solutes that poorly diffuse from the droplet surface, such as L-leucine, as shown in other studies [44,45]. However, it has also been observed that even highly soluble molecules can form hollow particles at high evaporation rates [38]. The sunken depressions observed on the surfaces of formed mannitol/dextran particles by SEM in Figure 5 are characteristic of such hollow structures, and thus larger in size than particles with a compact core. Overall, higher inlet temperatures promote the formation of larger and more hollow particles. Conversely, low inlet temperatures facilitate slower drying, which is more likely to produce denser particles. However, low temperatures are less efficient at drying the formed particles, and thus results in higher residual moisture contents. Water is a plasticizer to the matrix ingredients used here, depressing the glass transition temperature and promoting

particles to bind together should they collide [46]. The overall effect for low inlet temperatures is the production of aggregated particles. Some of the large aggregates that are formed from low temperature drying are shown in Figure 6.

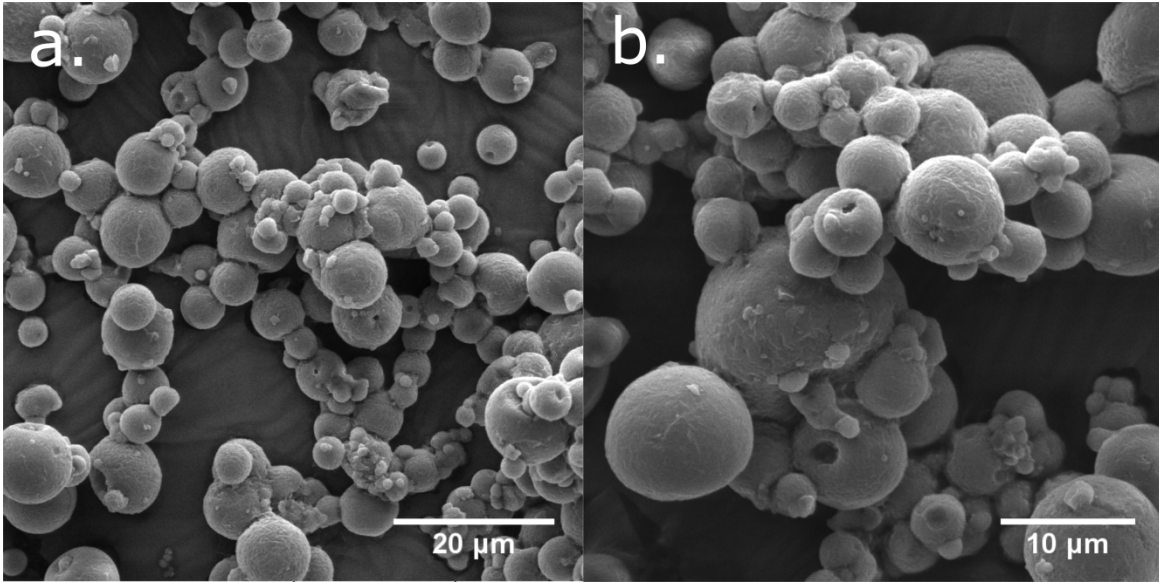


Figure 5. Spray dried particles (without AdHu5LacZ) formed at an inlet temperature of 150°C as imaged by SEM at (a) 3000x and (b) 5000x magnification. Significant bridging between particles is observed.

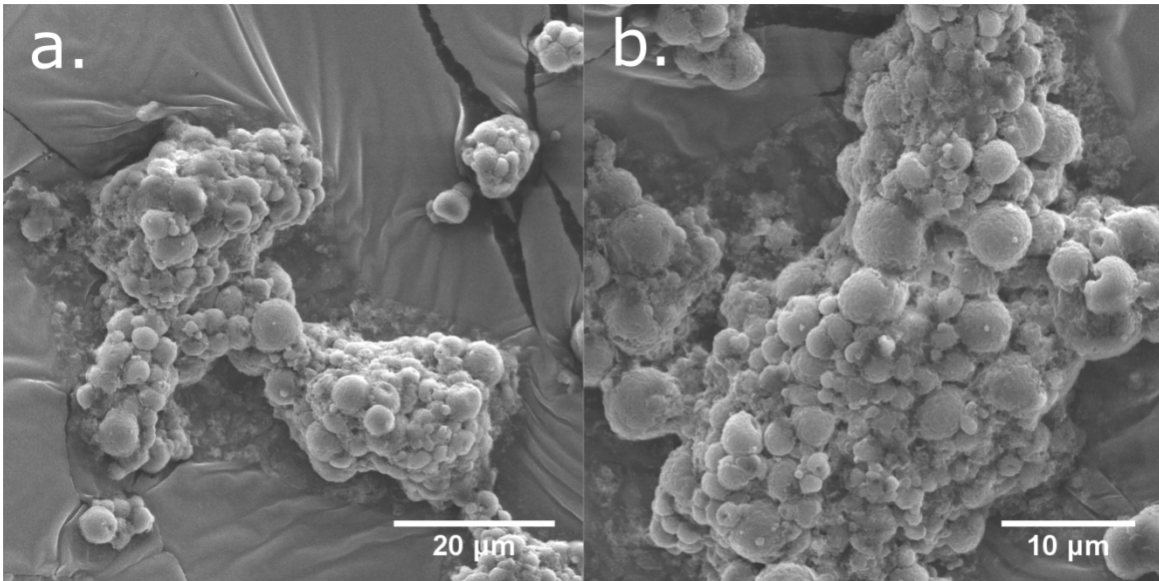


Figure 6. Spray dried particles (without AdHu5LacZ) formed at an inlet temperature of 90°C as imaged by SEM at (a) 3000x and (b) 5000x magnification. Particles adhere to each other due to incomplete powder drying.

Our results indicate that gas flow is linearly related to $F_{1-5\mu m}$. Hede et al. have demonstrated this relationship through the Weber number (We) where larger Weber numbers result in smaller sized particles [47]. The increased inertial terms of the Weber number caused by higher gas velocity is more likely to overcome the surface energy of the fluid to produce smaller droplets and hence smaller dry particles.

A second-order relationship was found between $F_{1-5\mu m}$ and the liquid feed rate (Figures 1a, b, d) with a minimum determined within the range of tested conditions. At low feed rates, a smaller amount of liquid is dispersed to form smaller droplets [48]. The trend resembles previous work modeling an exponential decrease in formed droplet size from an atomizer as the liquid feed to the system is reduced [47]. Increasing feed rate based on this theory should form large droplets; however, another phenomenon which begins to dominate causes this trend to gradually reverse. At a constant solute concentration, the larger particles are more hollow with a thinner shell than particles formed from smaller droplets [38]. The result is particles more prone to collapsing and breaking, which produces smaller-sized particles. These particles are shown in Figure 7, where the appearance of broken particles presumably leads to the creation of finer-sized debris. A single collapse/break can form many smaller particles, and thus the percentage of particles between 1 and 5 microns increases at high feed rates. Particle size data shown in Figure 4b indicates that such breakage can lead to a bimodal distribution.

It is known that a higher feed rate also corresponds to a lower outlet temperature within the spray dryer [49], which would indicate lower Peclet number drying. It was generally measured, and observed in Figure 7, that the effect of a high feed rate was more significant in producing hollow particles than the lower Peclet number drying was in preventing them.

However, the mentioned influence of the feed rate on the drying temperature seems present in the interaction parameter $TE \cdot F$ and so was a significant contributing effect overall (Table 2). Thus the formation of larger, more hollow particles (and smaller particles, through the collapse of these larger particles) results from a balance between the large droplets formed at high feed rates and the lower Peclet number drying (which promotes fewer hollow particles). The interaction parameter explains the small minima present when adjusting the feed rate or increasing inlet temperatures for a fixed feed rate. This reduction in $F_{1-5\mu m}$ is presumably due to less collapsed particles on account of the change in Peclet drying induced by the change in the feed flow rate.

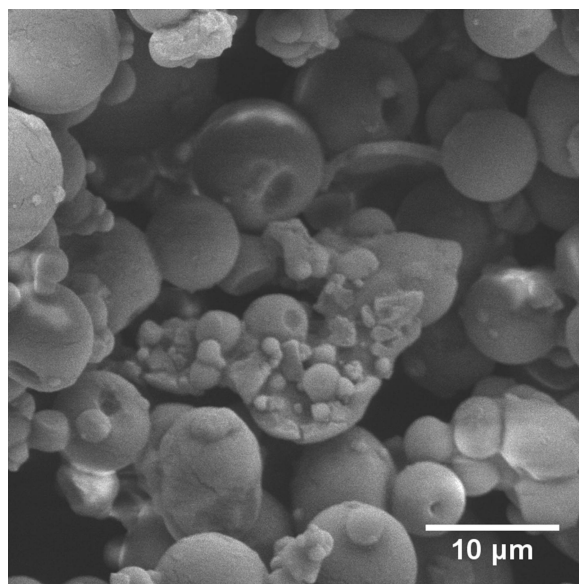


Figure 7. Spray dried particles (without AdHu5LacZ) formed at the high liquid feed rate imaged by SEM at 5000x magnification.

The solute concentration has a simple linear effect on $F_{1-5\mu m}$, like gas flow rate, with fewer particles of ideal size occurring due to preferential growth as the solute concentration was increased. This is related to the gradient in solute concentration radially within the droplet and a

receding capacity for solute to diffuse to the centre as the droplet shrinks through evaporation [42,50].

4.3. Powder Yield

The response surface with respect to powder yield shows similar trends to $F_{1-5\mu m}$ for the most significant processing parameters. Yield displays a simple linear dependency on inlet temperature, decreasing yield as TE increases, despite the non-negligible interaction terms for inlet temperature with solute concentration and feed rate (Equation 2). The increased likelihood of particle bridging with increased inlet temperature mentioned in Section 4.2 (and shown in Figure 5) will similarly result in more particles adhering to the spray chamber wall. By sticking to the wall, less powder was collected from the separating cyclone and hence yield decreased.

A second-order relationship exists for feed rate with a displayed maximum in the range of tested conditions. Yields decrease at higher and lower feed rates due to particle adherence to the spray dryer glassware. At low feed rates, there is less liquid for evaporation within the drying chamber, thus raising temperatures within the spray drying glassware [49]. Higher drying temperatures results in more free-flowing and adhering particles due to the particle T_g . Higher feed rates lower the temperature within the spray dryer, but also increases the moisture content of the particles [51,52]. Greater particle water content reduces the matrix T_g , thus although the temperature within the spray dryer is lower, the temperature at which the particles become sticky and free flowing is also lower. Sticky and free flowing particles readily adhere to the spray dryer chamber walls, reducing powder yield. Similar particle adherence has previously been observed in studies by Bowen et al. and Gikanga et al. with the use of benchtop- and industrial-sized spray dryers [53,54]. Our work agrees with the conclusions by Bowen et al. and Gikanga et al. in comparing bench top- and industrial-sized spray drying, highlighting that powder yield is

majorly impacted by adherence of spray dried particles to the glass chambers. Thus our findings can be appropriately scaled to apply to larger spray dryer units. These effects are further evident from the interaction between inlet temperature and feed rate ($TE \cdot F$, Figure 2b). At the maximum for each of these conditions, both spray dryer temperature and particle moisture are elevated. The reduced glass transition temperature of these particles at high temperatures causes the greatest particle adherence, and greatest loss of yield.

Interaction between the feed rate and solid matrix concentration ($F \cdot S$) is shown in Figure 2a. The yield exhibits a parabolic dependency on the feed rate, as discussed previously. Increasing the solute concentration increases the feed rate at which the maximum yield occurs, meaning optimal powder yields occur at higher feed rates for higher matrix solid concentrations, and at lower feed rates for lower matrix solid concentrations. This is not a major shift, as the optimal powder yield feed rate at the lowest and greatest matrix solid concentrations is approximately 190 mL/h and 230 mL/h, respectively, indicating only a modest change in feed rate for varying matrix solid concentrations. This small variation is likely a result of the thermal property changes at these conditions. As described, major powder losses occur due to powder adhering to the wall of the spray drying chambers, which occurs at temperatures approaching or above the particle T_g . Increasing matrix solid concentration reduces the amount of remaining moisture in a formed particle by increasing the ratio of precipitating solute to water per drying droplet. This change in moisture content increases the particle T_g and thus shifts the feed rate necessary for optimal powder yield, as observed in Figure 2a.

It is also of important note that yield can be greatly affected by the efficiency of the separating cyclone used. Bowen et al. have previously demonstrated in detail that greater yields

can be accomplished through use of a different cyclone [53]. Within this report, a high efficiency cyclone was used in order to best collect small-sized particles.

4.4. Titre Loss

To understand the influence of spray drying parameters on the observed loss in viral activity, it is important to understand the many routes, both physical and chemical, that can lead to adenovirus deactivation. To retain activity, the virus must maintain its structure and stay intact, which requires that the viral proteins preserve their primary, secondary, tertiary and quaternary structure [55,56]. Protein unfolding and denaturation can occur chemically through protein interactions with hydrophobic surfaces (including the air-water interface) leading to changes in secondary and tertiary structure [4,5] thus water replacement by the excipient formulation is necessary through drying to maintain a hydrophilic environment. Protein aggregation and protein unfolding due to elevated temperature are other common routes to deactivation where protein function is lost by being in the denatured state [57–60]. Losses of viral activity can also occur from physical forces, such as high shear, which can mechanically disrupt/damage the virus particles [61–63]. Thus minimal AdHu5LacZ titre loss is achieved by preventing chemical, thermal and physical inactivation.

Adjusting the inlet temperature within the spray dryer controls the total energy in the drying system. Thus, the inlet temperature, as set by the temperature of the spray nozzle, is a very important parameter, and was determined to be the only factor that was significant for all three responses. Increasing this temperature increases the drying rate of the particles but also the free energy for deformation/protein denaturation of a labile material such as the viral vector. This is seen experimentally as an increase in the total titre loss of AdHu5LacZ with increasing inlet

temperature, which generally agrees with bench top studies of protein denaturation as a function of temperature [4,64]. While high inlet temperatures are not optimal for powder yield or particles of ideal size either, there is still a lower bound to the inlet temperature because particle development (i.e. formation of dry particles, overall powder yield, etc.) will also be negatively affected.

Increasing gas flow rate during spray drying increases the total titre loss (Figures 3d, e, and f). A larger gas flow rate increases the shear applied to the liquid feed, breaking the liquid into smaller-sized droplets and correspondingly, increases the total air-water interface which decreases vector stability. The amount of shear ($\dot{\gamma}$) applied to the fluid in a two-fluid nozzle atomizer is estimated through Equation 6, where U_{av} refers to the average velocity of the spray gas and liquid feed, U_l refers to the velocity of the liquid feed and D_L refers to the diameter of the spray nozzle[47].

$$\dot{\gamma} \approx \frac{2(U_{av} - U_l)}{D_L} \quad (6)$$

Previous work has shown that protein denaturation can be related to shear forces on biological compounds, such as work by Maa and Hsu observing changes in protein conformation by high shear mixers and work by Ghandi et al. demonstrating reduced survival of *Lactococcus lactis* at greater spray dryer shear rates[61,65]. The trend observed in those studies showed that biological activity decreased exponentially for increasing shear rates. Our study does not have a sufficient number of gas flow rates to fully model an exponential trend but we do find a second-order dependency as denoted by the significant model terms being SG and SG•SG in Equation 3 and displayed in Figures 3d, e, and f. The increase in air-water interfacial area resulting from

smaller droplet sizes at high shear rates is further detrimental to native protein structure as these interfaces act as hydrophobic “surfaces” and enhance the rate of protein denaturing [5,62]. Maa and Hsu have previously demonstrated that the rate of protein denaturation is increased through the combined effect of shear and air-water interface[62]. As proteins are amphiphilic molecules, air-water interfaces can lead to denaturing by exposing hydrophobic moieties. Thus an increase in spray gas flow rate leading to a finer spray increases the rate of denaturing for viral vector proteins.

Increasing the feed rate will increase shear forces within the nozzle, but as indicated by Equation 6, increasing feed rate will actually decrease the apparent shear rate on droplets formed at the end of the nozzle at a given gas flow rate. Due to the loss in viral vector activity by increased shear from spray gas flow rates, the expectation is a reduction in titre loss at high flow rates. However, feed rate is not a significant term in Equation 3. This is due to the differences in magnitude between the spray gas flow rate and liquid feed rate. Overall, there was no observed effect on the total titre loss by adjusting the feed flow rate to the nozzle, indicating minimal influence of this variable relative to the other contributing parameters of inlet temperature and gas flow rate (Table 2).

In this work, a blend of mannitol and dextran is chosen as a good excipient matrix for thermal stabilization of viral vectors based on our previous study which thoroughly investigated matrix properties and their effect on long term storage of AdHu5 at high temperatures [15]. Changing the matrix solute concentration in the feed will primarily affect the ability for the matrix to encapsulate the bioactive agent which is required to retain bioactivity. Stabilization of other virus types has also been demonstrated through spray drying with sugar matrices [66,67]. As predicted, the total titre loss is lowered by increasing the matrix solute concentration in the

liquid feed (Table 2). The natural state for AdHu5 is within an aqueous environment where hydrogen bonding with water molecules maintains proper protein structure [68,69]. Thus viral vector protein denaturation can occur throughout drying due to the loss of water molecules [70]. Matrix solutes are able to replace these stabilizing interactions and prevent a loss of protein structure during drying [20,71]. This explains the preference of hydrogen-bonding molecules, such as carbohydrates, for stabilization of biological materials through vitrification [72]. Greater amounts of hydrogen-bonding molecules, such as mannitol and dextran, within the drying droplets impart a greater stability on the viral vector due to the increase in potential for hydrogen-bonding, and thus better maintaining a hydrophilic environment. The greatest viral vector stabilization is achieved at the greatest feed matrix concentration. However, at high liquid feed rates, the solute concentration has a negligible effect on the AdHu5 titre loss (Figure 3a). This is represented by the interaction parameter for liquid feed rate and solute concentration (F•S) in Table 2. High feed rates correspond to higher retention of water within spray dried particles. The requirement for water replacing bonds is lower in particles that retain water.

4.5. Significance of Findings

A summary of our findings is presented in Figure 8 to highlight the complex nature of the dependent parameters. All three responses cannot be maximized within a given set of processing conditions which then require the outputs to be prioritized. Furthermore, while some trends may seem obvious (i.e. a decrease in viral vector activity for higher spray drying temperatures), it is not obvious to which magnitude these effects are present and how they correlate to other responses. To expand upon this, the incorporation of a labile material requires that titre loss be minimized – most users will agree that this is the primary constraint given the high cost of

producing, for example, viral vectors. Process yield and particle size can then be optimized as secondary parameters depending on matrix material and processing costs and the intended method of delivery of the API. Figure 8 shows that careful optimization of one parameter will result in suboptimal values for the other responses. For example, increasing the solute concentration decreases the loss of the viral vector through spray drying, but also decreases the powder yield and amount of particles in the desired size range. A good compromise for all three responses could be to spray dry with medium-low inlet temperature, medium spray gas flow rate, medium feed rate, and high solute concentration noting that inlet temperature and gas flow are the most influential parameters

While the exact responses will differ for different formulations and spray dryer setups, the trends and interactions outlined and discussed here can serve as a guide for future investigations. The use of dimensionless numbers allows the findings discussed here to be scaled up appropriately. For example, as previously discussed, work by Gikanga et al. and Bowen et al. has highlighted similar trends in terms of powder yield for a high throughput spray dryer [53,54]. The results are intended to emphasize why optimization studies are needed with the vaccine platform present and that focusing only on a specific response, such as particle size, can be detrimental towards the overall purpose (i.e., optimizing particle size in this system would lead to a reduction in powder yield and viral vector activity).

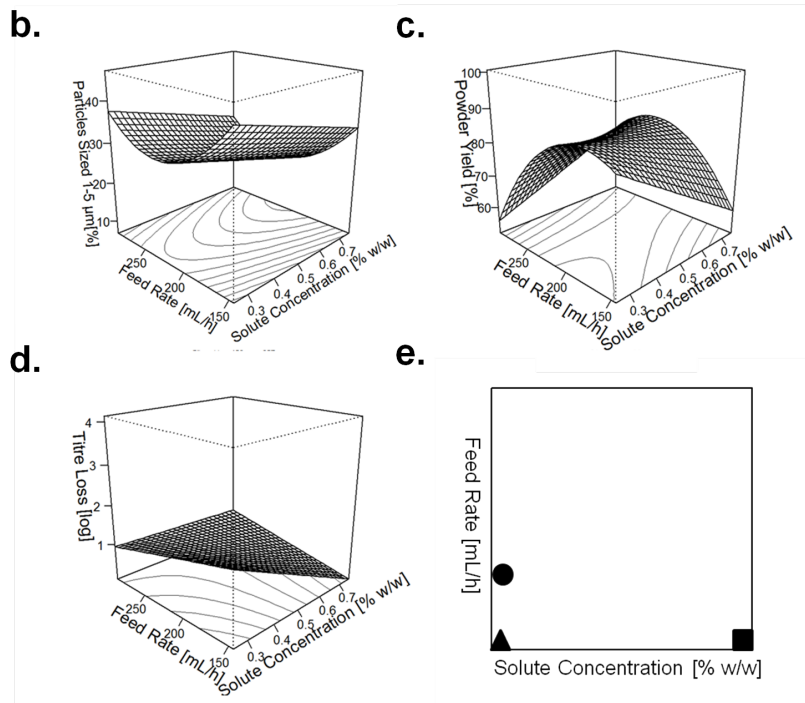
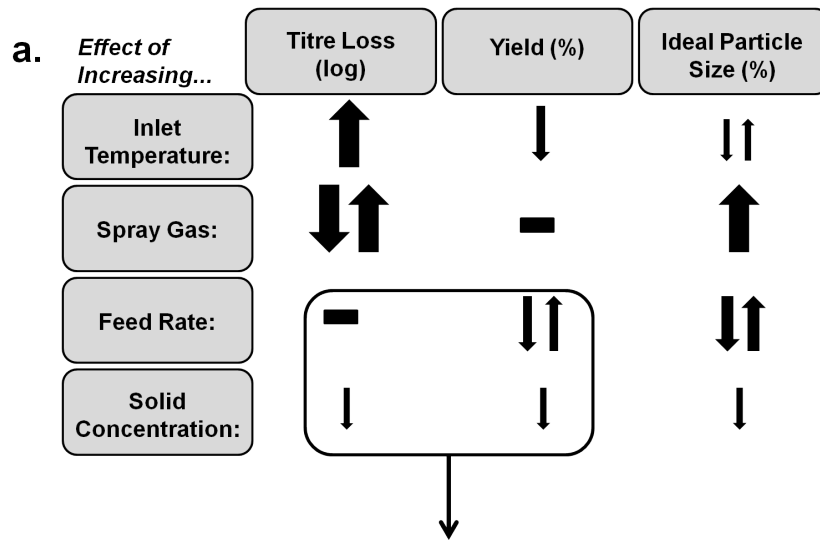


Figure 8. a) Effect of input parameters (inlet temperature, spray gas flow, feed rate, matrix solid concentration) on the viral vector titre loss (log), powder yield (%) and the percentage of ideally sized particles (%). The magnitude of the effect is demonstrated by the thickness of the arrow. Below are plots demonstrating differences between b) particles sized 1-5 μm , c) powder yield and d) titre loss. e) This is highlighted in the two dimensional plot, showing optima for particles sized 1-5 μm (\blacktriangle), powder yield (\bullet) and titre loss (\blacksquare).

5. CONCLUSIONS

Overall, this work highlights the importance of including the vector platform while seeking optimal spray drying parameters for this new class of thermally stable vaccines and demonstrates for the first time the effects of spray drying parameters on viral vector activity. The statistical models constructed suggest that the spray drying process can be adjusted to account for control over each of the three measured responses, however it also emphasizes the competing nature in optimizing for any particular response. Optimal output of one specific response can lead to significant loss in the other responses. The responses to each process parameter change can perhaps be estimated through known theory, though the magnitudes of each effect is nontrivial. Overall, the results presented can be applied to current spray drying processes, both laboratory- and industry-scale, to develop desirable particle properties for all three responses. While new processes may use different excipients with a different labile material than what was used here, the trends and interactions remain constant, proving to be a valuable asset for future studies.

6. ACKNOWLEDGEMENTS

The authors thank Dr. Pelton for equipment use and Anna Zganiacz and Xueya Feng for cell culture training and general assistance. The authors would also like to thank both the Canadian Centre for Electron Microscopy and the Biointerfaces Institute for use of their facilities. This study is supported by funds from the Canadian Institutes of Health Research and Natural Sciences and Engineering Research Council of Canada.

7. REFERENCES

1. Brandau DT, Jones LS, Wiethoff CM, Rexroad J, Middaugh CR. Thermal Stability of Vaccines. *J. Pharm. Sci.* 2003;92:218–31.
2. Sovizi MR. Thermal behavior of drugs : Investigation on decomposition kinetic of naproxen and celecoxib. *J. Therm. Anal. Calorim.* 2010;102:285–9.
3. Craig DQ, Royall PG, Kett VL, Hopton ML. The relevance of the amorphous state to pharmaceutical dosage forms: glassy drugs and freeze dried systems. *Int. J. Pharm.* [Internet]. 1999;179:179–207. Available from: <http://www.ncbi.nlm.nih.gov/pubmed/10053213>
4. Dill K a, Shortle D. Denatured states of proteins. *Annu. Rev. Biochem.* 1991;60:795–825.
5. Tanford C. Contribution of hydrophobic interactions to the stability of the globular conformation of proteins. *J. Am. Chem. Soc.* 1962;84:4240.
6. Bishara RH. Cold chain management—an essential component of the global pharmaceutical supply chain. *Am. Pharm. Rev.* [Internet]. 2006;9:105–9. Available from: <http://www.sensitech.com.mx/assets/articles/lbsharaapr.pdf>
7. Croyle M a, Roessler BJ, Davidson BL, Hilfinger JM, Amidon GL. Factors that influence stability of recombinant adenoviral preparations for human gene therapy. *Pharm. Dev. Technol.* [Internet]. 1998;3:373–83. Available from: <http://www.ncbi.nlm.nih.gov/pubmed/9742558>
8. Rexroad J, Evans RK, Middaugh CR. Effect of pH and ionic strength on the physical stability of adenovirus type 5. *J. Pharm. Sci.* [Internet]. 2006 [cited 2015 Mar 30];95:237–47. Available from: <http://www.ncbi.nlm.nih.gov/pubmed/16372304>
9. Sprangers MC, Lakhai W, Koudstaal W, Verhoeven M, Koel BF, Vogels R, et al. Quantifying Adenovirus-Neutralizing Antibodies by Luciferase Transgene Detection: Addressing Preexisting Immunity to Vaccine and Gene Therapy Vectors. *J. Clin. Microbiol.* 2003;41:5046–52.
10. Elzey BD, Siemens DR, Ratliff TL, Lubaroff DM. Immunization with type 5 adenovirus recombinant for a tumor antigen in combination with recombinant canarypox virus (ALVAC) cytokine gene delivery induces destruction of established prostate tumors. *Int. J. Cancer* [Internet]. 2001;94:842–9. Available from: <http://www.ncbi.nlm.nih.gov/pubmed/11745487>
11. Desobry S a, Netto FM, Labuza TP. and Freeze-drying for b -Carotene Encapsulation and Preservation INTRODUCTION. *J. Food Sci.* 1997;62:1158–62.
12. Sollohub K, Cal K. Spray Drying Technique: II. Current Applications in Pharmaceutical Technology. *J. Pharm. Sci.* [Internet]. 2010;99:587–97. Available from: <http://linkinghub.elsevier.com/retrieve/pii/S0022354916304129>
13. Vehring R. Pharmaceutical particle engineering via spray drying. *Pharm. Res.* 2008;25:999–1022.
14. Abdul-Fattah AM, Truong-Le V, Yee L, Pan E, Ao Y, Kalonia DS, et al. Drying-induced variations in physico-chemical properties of amorphous pharmaceuticals and their impact on Stability II: stability of a vaccine. *Pharm. Res.* [Internet]. 2007 [cited 2014 Mar 26];24:715–27. Available from: <http://www.ncbi.nlm.nih.gov/pubmed/17372697>

15. LeClair DA, Cranston ED, Xing Z, Thompson MR. Evaluation of excipients for enhanced thermal stabilization of a human type 5 adenoviral vector through spray drying. *Int. J. Pharm.* [Internet]. Elsevier B.V.; 2016;506:289–301. Available from: <http://linkinghub.elsevier.com/retrieve/pii/S0378517316303507>
16. Gibbs BF, Kermasha S, Alli I, Mulligan CN. Encapsulation in the food industry: a review. *Int. J. Food Sci. Nutr.* [Internet]. 1999;50:213–24. Available from: <http://www.ncbi.nlm.nih.gov/pubmed/10627837>
17. Broadhead J, Edmond Rouan SK, Rhodes CT. The spray drying of pharmaceuticals. *Drug Dev. Ind. Pharm.* [Internet]. 1992;18:1169–206. Available from: <http://www.tandfonline.com/doi/full/10.3109/03639049209046327>
18. Thybo P, Hovgaard L, Lindeløv JS, Brask A, Andersen SK. Scaling up the spray drying process from pilot to production scale using an atomized droplet size criterion. *Pharm. Res.* 2008;25:1610–20.
19. Crowe LM, Crowe JH, Rudolph A, Womersley C, Appel L. Preservation of freeze-dried liposomes by trehalose. *Arch. Biochem. Biophys.* 1985;242:240–7.
20. Crowe LM, Reid DS, Crowe JH. Is trehalose special for preserving dry biomaterials? *Biophys. J.* [Internet]. Elsevier; 1996;71:2087–93. Available from: [http://dx.doi.org/10.1016/S0006-3495\(96\)79407-9](http://dx.doi.org/10.1016/S0006-3495(96)79407-9)
21. Bhandari BR, Howes T. Implication of glass transition for the drying and stability of dried foods. *J. Food Eng.* 1999;40:71–9.
22. World Health Organization. Global Vaccine Action Plan 2011-2020. WHO; 2011. p. 1–147.
23. Maury M, Murphy K, Kumar S, Shi L, Lee G. Effects of process variables on the powder yield of spray-dried trehalose on a laboratory spray-dryer. *Eur. J. Pharm. Biopharm.* 2005;59:565–73.
24. Elversson J, Millqvist-Fureby A. Particle size and density in spray drying-effects of carbohydrate properties. *J. Pharm. Sci.* 2005;94:2049–60.
25. Grabowski JA, Truong VD, Daubert CR. Spray-drying of amylase hydrolyzed sweetpotato puree and physicochemical properties of powder. *J. Food Sci.* 2006;71.
26. Eldem T, Speiser P, Hincal A. Optimization of Spray-Dried and -Congealed Lipid Micropellets and Characterization of Their Surface Morphology by Scanning Electron Microscopy. *Pharm. Res. An Off. J. Am. Assoc. Pharm. Sci.* 1991. p. 47–54.
27. To BCS, Etzel MR. Spray Drying, Freeze Drying, or Freezing of Three Different Lactic Acid Bacteria Species. *J. Food Sci.* [Internet]. 1997;62:576–8. Available from: <http://doi.wiley.com/10.1111/j.1365-2621.1997.tb04434.x>
28. Adjallé KD, Vu KD, Tyagi RD, Brar SK, Valéro JR, Surampalli RY. Optimization of spray drying process for *Bacillus thuringiensis* fermented wastewater and wastewater sludge. *Bioprocess Biosyst. Eng.* 2011;34:237–46.
29. Prabakaran G, Hoti SL. Optimization of spray-drying conditions for the large-scale preparation of *Bacillus thuringiensis* var. *israelensis* after downstream processing. *Biotechnol.*

Bioeng. 2008;100:103–7.

30. Amaro MI, Tajber L, Corrigan OI, Healy AM. Optimisation of spray drying process conditions for sugar nanoporous microparticles (NPMs) intended for inhalation. *Int. J. Pharm.* 2011;421:99–109.
31. Billon A, Bataille B, Cassanas G, Jacob M. Development of spray-dried acetaminophen microparticles using experimental designs. *Int. J. Pharm.* 2000;203:159–68.
32. Jensen DMK, Cun D, Maltesen MJ, Frokjaer S, Nielsen HM, Foged C. Spray drying of siRNA-containing PLGA nanoparticles intended for inhalation. *J. Control. Release.* 2010;142:138–45.
33. Audouy SAL, van der Schaaf G, Hinrichs WLJ, Frijlink HW, Wilschut J, Huckriede A. Development of a dried influenza whole inactivated virus vaccine for pulmonary immunization. *Vaccine.* 2011;29:4345–52.
34. Xing Z, Ohkawara Y, Jordana M, Graham FL, Gauldie J. Transfer of Granulocyte-Macrophage Colony-stimulating Factor Gene to Rat Lung Induces Eosinophilia, Monocytosis, and Fibrotic Reactions. *J. Clin. Invest.* 1996;97:1102–10.
35. Prinn KB, Costantino HR, Tracy M. Statistical modeling of protein spray drying at the lab scale. *AAPS PharmSciTech.* 2002;3:E4.
36. Oakley DDE. Spray Dryer Modeling in Theory and Practice. *Dry. Technol.* [Internet]. 2004;22:1371–402. Available from: <http://dx.doi.org/10.1081/DRT-120038734>\n<http://www.tandfonline.com/doi/abs/10.1081/DRT-120038734?src=recsys#.VbIyxPmqkko>\n<http://www.tandfonline.com/doi/pdf/10.1081/DRT-120038734>
37. Abràmoff MD, Magalhães PJ, Ram SJ. Image processing with imageJ. *Biophotonics Int.* 2004;11:36–41.
38. Elversson J, Millqvist-Fureby A, Alderborn G, Elofsson U. Droplet and particle size relationship and shell thickness of inhalable lactose particles during spray drying. *J. Pharm. Sci.* 2003;92:900–10.
39. Dixon WJ. Analysis of Extreme Values. *Ann. Math. Stat.* 1950;21:488–506.
40. Reed L, Muench H. A simple method of estimating fifty per cent endpoints. *Am. J. Epidemiol.* 1938;27:493–7.
41. Roos YH. Importance of glass transition and water activity to spray drying and stability of dairy powders. *Lait.* 2002;82:475–84.
42. Vehring R, Foss WR, Lechuga-Ballesteros D. Particle formation in spray drying. *J. Aerosol Sci.* 2007;38:728–46.
43. Winterton RHS. Newton’s law of cooling. *Contemp. Phys.* [Internet]. 1999;40:205–12. Available from: <http://www.tandfonline.com/doi/abs/10.1080/001075199181549>
44. Najafabadi AR, Gilani K, Barghi M, Rafiee-Tehrani M. The effect of vehicle on physical properties and aerosolisation behaviour of disodium cromoglycate microparticles spray dried alone or with L-leucine. *Int. J. Pharm.* 2004;285:97–108.

45. Aquino RP, Prota L, Auriemma G, Santoro a., Mencherini T, Colombo G, et al. Dry powder inhalers of gentamicin and leucine: Formulation parameters, aerosol performance and in vitro toxicity on CuFi1 cells. *Int. J. Pharm.* 2012;426:100–7.
46. Hancock BC, Zografi G. The Relationship Between the Glass Transition Temperature and the Water Content of Amorphous Pharmaceutical Solids. *Pharm. Res.* 1994;11:471–7.
47. Hede PD, Bach P, Jensen AD. Two-fluid spray atomisation and pneumatic nozzles for fluid bed coating/agglomeration purposes: A review. *Chem. Eng. Sci.* 2008;63:3821–42.
48. Lin SP, Reitz RD. Drop and Spray Formation From a Liquid Jet. *Annu. Rev. Fluid Mech.* 1998;30:85–105.
49. Maa YF, Costantino HR, Nguyen P a, Hsu CC. The effect of operating and formulation variables on the morphology of spray-dried protein particles. *Pharm. Dev. Technol.* 1997;2:213–23.
50. Huang D. Modeling of Particle Formation During Spray Drying. *Eur. Dry. Conf.* Palma, Spain; 2011.
51. Joo HH, Yong HC. Physico-chemical properties of protein-bound polysaccharide from *Agaricus blazei* Murill prepared by Ultrafiltration and spray drying process. *Int. J. Food Sci. Technol.* [Internet]. 2007;42:1–8. Available from: <http://www.scopus.com/inward/record.url?eid=2-s2.0-33845967797&partnerID=40&md5=94d5191b29ee5d659e4699d6477f42cf>
52. Tonon R V., Brabet C, Hubinger MD. Influence of process conditions on the physicochemical properties of açai (*Euterpe oleraceae* Mart.) powder produced by spray drying. *J. Food Eng.* [Internet]. 2008;88:411–8. Available from: <http://linkinghub.elsevier.com/retrieve/pii/S0260877408001179>
53. Bowen M, Turok R, Maa Y-F. Spray Drying of Monoclonal Antibodies: Investigating Powder-Based Biologic Drug Substance Bulk Storage. *Dry. Technol.* [Internet]. 2013;31:1441–50. Available from: <http://www.tandfonline.com/doi/abs/10.1080/07373937.2013.796968>
54. Gikanga B, Turok R, Hui A, Bowen M, Stauch OB, Maa Y-F. Manufacturing of High-Concentration mAb Formulations via Spray Drying - the Road to Manufacturing Scale. *PDA J. Pharm. Sci. Technol.* [Internet]. 2015;69:59–73. Available from: http://www.spxflow.com/en/assets/pdf/PDA_#1003_-_Manufacturing_of_High-Concentration_mAb_Formulations_via_Spray_Drying_tcm11-55210.pdf
55. Klein H, Maltzman W, Levine AJ. Structure-Function Relationships of the Adenovirus DNA-binding Protein. *J. Biol. Chem.* 1979;254:11051–60.
56. Norrby E. The structural and functional diversity of adenovirus capsid components. *J. Gen. Virol.* 1969;5:221–36.
57. Ihnat PM, Vellekamp G, Obenauer-Kutner LJ, Duan J, Han M a, Witchey-Lakshmanan LC, et al. Comparative thermal stabilities of recombinant adenoviruses and hexon protein. *Biochim. Biophys. Acta* [Internet]. 2005 [cited 2015 Mar 30];1726:138–51. Available from: <http://www.ncbi.nlm.nih.gov/pubmed/16023295>
58. Baldwin RL. Temperature Dependence of the Hydrophobic Interaction in Protein Folding.

- Proc. Natl. Acad. Sci. [Internet]. 1986;83:8069–72. Available from:
<http://www.pubmedcentral.nih.gov/articlerender.fcgi?artid=386868&tool=pmcentrez&rendertype=abstract>
<http://www.pnas.org/content/83/21/8069.short>
59. Day R, Bennion BJ, Ham S, Daggett V. Increasing temperature accelerates protein unfolding without changing the pathway of unfolding. *J. Mol. Biol.* 2002;322:189–203.
60. Monahan FJ, German JB, Kinsellat JE. Effect of pH and Temperature on Protein Unfolding and Thiol / Disulfide Interchange Reactions during Heat-Induced Gelation of Whey Proteins. *J. Agric. Food Chem.* 1995;43:46–52.
61. Maa Y-F, Hsu CC. Effect of High Shear on Proteins. *Biotechnol. Bioeng.* 1996;51:458–65.
62. Maa YF, Hsu CC. Protein denaturation by combined effect of shear and air-liquid interface. *Biotechnol. Bioeng.* 1997;54:503–12.
63. D'Souza DH, Su X, Roach A, Harte F. High-pressure homogenization for the inactivation of human enteric virus surrogates. *J. Food Prot.* 2009;72:2418–22.
64. Dill KA. Dominant Forces in Protein Folding. *Biochemistry.* 1990;29:7133–55.
65. Ghandi A, Powell IB, Howes T, Chen XD, Adhikari B. Effect of shear rate and oxygen stresses on the survival of *Lactococcus lactis* during the atomization and drying stages of spray drying: A laboratory and pilot scale study. *J. Food Eng.* [Internet]. Elsevier Ltd; 2012;113:194–200. Available from: <http://dx.doi.org/10.1016/j.jfoodeng.2012.06.005>
66. Saluja V, Amorij JP, Kapteyn JC, de Boer a. H, Frijlink HW, Hinrichs WLJ. A comparison between spray drying and spray freeze drying to produce an influenza subunit vaccine powder for inhalation. *J. Control. Release* [Internet]. Elsevier B.V.; 2010;144:127–33. Available from: <http://dx.doi.org/10.1016/j.jconrel.2010.02.025>
67. Ré MI. Microencapsulation By Spray Drying. *Dry. Technol.* 1998;16:1195–236.
68. Tarek M, Tobias DJ. Role of protein-water hydrogen bond dynamics in the protein dynamical transition. *Phys. Rev. Lett.* 2002;88:138101.
69. Ippolito JA, Alexander RS, Christianson DW. Hydrogen bond stereochemistry in protein structure and function. *J. Mol. Biol.* 1990. p. 457–71.
70. Prestrelski SJ, Tedeschi N, Arakawa T, Carpenter JF. Dehydration-induced conformational transitions in proteins and their inhibition by stabilizers. *Biophys. J.* [Internet]. 1993;65:661–71. Available from:
<http://www.pubmedcentral.nih.gov/articlerender.fcgi?artid=1225768&tool=pmcentrez&rendertype=abstract>
71. Liao Y-H, Brown MB, Nazir T, Quader A, Martin GP. Effects of sucrose and trehalose on the preservation of the native structure of spray-dried lysozyme. *Pharm. Res.* [Internet]. 2002;19:1847–53. Available from: <http://www.ncbi.nlm.nih.gov/pubmed/12523664>
72. Amorij J-P, Huckriede A, Wilschut J, Frijlink HW, Hinrichs WLJ. Development of stable influenza vaccine powder formulations: challenges and possibilities. *Pharm. Res.* [Internet]. 2008 [cited 2014 Mar 23];25:1256–73. Available from:
<http://www.pubmedcentral.nih.gov/articlerender.fcgi?artid=2346510&tool=pmcentrez&rendertype=abstract>

pe=abstract